SAND2001-8012

Moody, N. R., Yang, N., Adams, D. P., Cordill, M. J., Bahr, D. F., (2002) The effects of copper on the interfacial fracture of gold films, In: *Thin Films-Stresses and Mechanical Properties IX* (edited by Ozkan, C. S., Camarata, R. C., Freund, L. B., Gao, H.) Materials Research Society, Pittsburgh, PA, **695**, L7.5.1-L7.5.6.

The Effects of Copper on the Interfacial Failure of Gold Films

N. R. Moody, D. P. Adams*, M. J. Cordill**, N. Yang, D. F. Bahr**
Sandia National Laboratories, Livermore, CA 94550
*Sandia National Laboratories, Albuquerque, NM 87185
**Washington State University, Pullman WA 99164

ABSTRACT

Nanoindentation test techniques were combined with deposition of highly stressed overlayers to study the interfacial fracture susceptibility of gold-on-copper and gold-2w/o-copper alloy films. The gold-on-copper film blistered readily following deposition of stressed tungsten overlayers. Additional stress from nanoindentation was required to trigger delamination and blister formation in the gold-copper alloy film. Fracture energies were then determined using mechanics-based models. The results show that the gold-copper alloy exhibited higher fracture energies than the gold-on-copper films. This increase scaled with film strength suggesting that the higher measured fracture energies in the gold-copper alloy film were due to solid solution hardening.

INTRODUCTION

Adhesion is an important factor in controlling the performance of thin film devices. [1,2] It is a critical factor in hybrid microcircuits where the diffusion of copper from leads during processing and service can degrade performance and reliability to unacceptable levels. [3-5] Close examination of microcircuits subjected to accelerated aging show significant levels of copper migration from the copper-cored-leads to the gold-conductive-pads. The gold pads become an essentially uniform solid solution of gold-2w/o-copper while copper concentrations along the lead-pad bond often exceed 20 w/o. However, there are no studies that provide a measure of how copper concentration affects interfacial fracture of gold films nor are there studies that correlate fundamental results to microcircuit performance and reliability.

Traditional test techniques such as double cantilever beam sandwich samples often require relatively thick films while peel tests are dominated by plastic energy contributions as the film is bent. [6] The work of Bagchi et al. [7,8], and more recently the work by Kriese and coworkers [9,10] shows that these limitations can be overcome for testing thin metal films by deposition of a relatively hard highly stressed overlayer. This overlayer applies a uniform stress to the ductile films while constraining out-of-plane plasticity [7-10] In this study, we combined stressed overlayers with nanoindentation to study the effects of copper on the adhesion of gold films to sapphire substrates.

MATERIALS

The materials used in this study were thin gold-on-copper and gold-2w/o-copper films sputter deposited onto polished single crystal (0001) sapphire substrates. The substrates were prepared by ultrasonic cleaning in acetone for ten minutes, in ethyl alcohol for five minutes, and then in 1M HCl for five minutes. This was followed by rinses with de-ionized water and nitrogen gas. The substrates were then transferred to a deposition chamber and heated to 700˚C in vacuum for five minutes to drive off moisture and cooled to room temperature. The films were deposited on the substrates using gold, copper, and gold-2w/o-copper targets with argon as the carrier gas in a vacuum apparatus having a base pressure of 1.3×10^{-5} Pa (10^{-7} torr). For the gold-on-copper films, copper was deposited first to a thickness of 6 nm. This was followed by deposition of gold to a thickness of 200 nm. The gold-2w/o-copper films were deposited in a separate run to a thickness of 200 nm. All films were deposited at a nominal rate of 0.3 nm/s with final film thickness confirmed using a Tencor Profilometer.

Mechanical properties were determined for each multilayer film system using the continuous stiffness measurement option on a Nano Indenter II™ with a Berkovich diamond indenter. All measurements were conducted at an excitation frequency of 45 Hz and displacement of 3 nm.

Following nanoindentation testing, a tungsten overlayer was deposited on all films to provide a uniform compressive stress for fracture testing. Deposition was accomplished by placing the gold-on-copper and gold-2w/o-copper films in a sputter deposition chamber and heating to 170˚C in vacuum to drive off moisture. Cleaning was completed with an RF backsputter to remove contaminants from the surface. The tungsten films were deposited to a thickness of 840 nm at a rate of 0.3 nm/s using a tungsten target and 3.3 mtorr argon as the carrier gas in a vacuum system having a base pressure of 1.3×10^{-5} Pa (10^{-7} torr).

Resistance to fracture was determined from uniform width blisters which formed after deposition of the tungsten overlayers, and from circular blisters triggered by nanoindentation of blister-free regions. For the nanoindentation tests, a conical diamond indenter with a nominal one μm tip radius and a 90˚ included angle was driven into the films at a loading rate of 600 μN/s to maximum loads of 200, 400, and 600 mN. During each test, the normal loads and displacements were continuously recorded.

RESULTS AND DISCUSSION

Nanoindentation results are given in Figure 1 and show that the elastic moduli of both films at the surface are near 90 GPa, slightly higher than values for bulk gold. In contrast, the hardness differed significantly between the films with values near 200 MPa for gold-on-copper films and near 300 MPa for gold-2w/o copper films. The values for the gold-on-copper film are similar to those measured in sputter deposited gold films.

Deposition of highly compressed tungsten overlayers induced extensive telephone cord blistering in the gold-on-copper films. (Figure 2a) Additional stress from nanoindentation was required to induce delamination and formation of circular blisters in isolated areas of the as-deposited gold-2w/o-copper film. (Figure 2b) In all cases, fracture occurred along the film-substrate interfaces with no evidence of gold or copper left on the sapphire substrates.

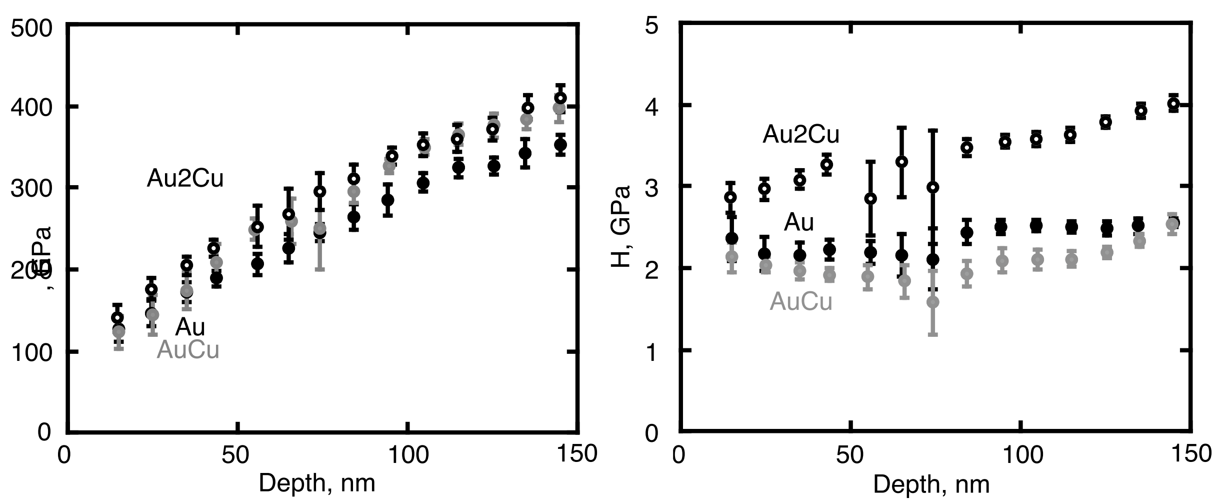

(a) (b)

Figure 1. (a) Elastic moduli extrapolate to surface values near 90 GPa for gold-on-copper, and gold-2w/o-copper films. (b) The hardness values average 2.2 GPa gold-on-copper films and 3.0 GPa for the gold-2w/o-copper film. The error bars correspond to one standard deviation. Values for sputter deposited gold films are included for comparison.

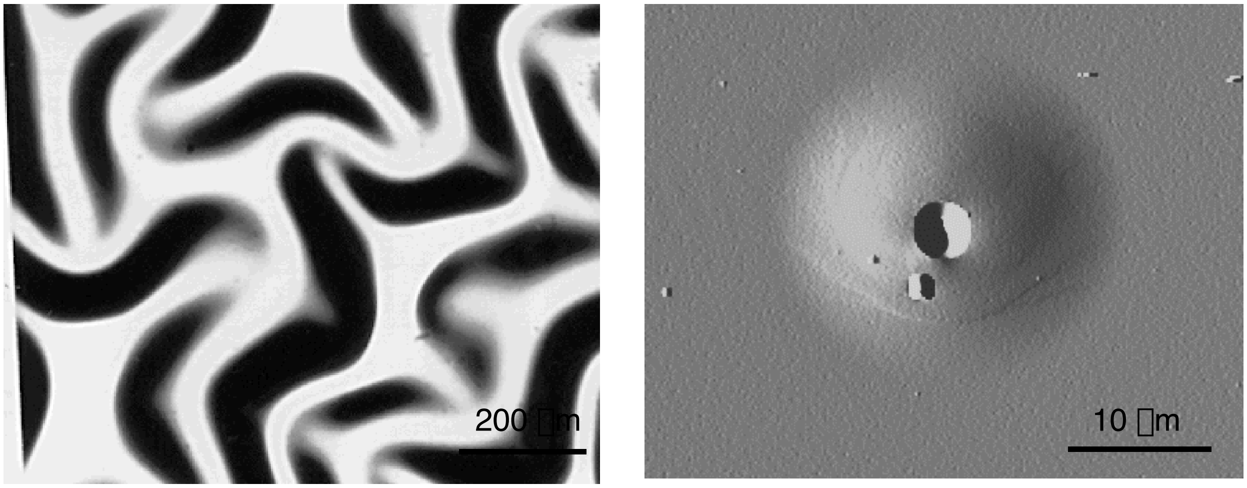

(a) (b)

Figure 2. Stressed overlayers triggered telephone cord blistering in the (a) gold-on-copper film. Additional stress from nanoindentation was needed to trigger (b) circular blister formation in the gold-2w/o-copper film.

The uniform width and circular blisters provide the data from which interfacial fracture energies can be obtained using solutions for film systems where residual stresses dominate fracture behavior. These solutions were originally derived for single layer film-on-substrate systems [11-13]. Work by Bagchi et al. [7,8] and more recently by Kriese et al. [9,10] extended these solutions to multilayer systems by treating the multilayer film as a single film of the same total thickness with a transformed moment of inertia. For a blister to form between the multilayer film and substrate, the compressive residual stress, σ_r, must exceed the stress for interfacial delamination, σ_b, as follows [9,11],

$$\sigma_b = \frac{\pi^2}{Bhb^2}\left(\frac{E_{Au}}{\left(1-\nu_{Au}^2\right)}\right)\left(I_T\right) \tag{1}$$

In this expression, I_T is the transformed moment of inertia for the multilayer film system [9], ν_{Au}, is Poisson's ratio for gold, b is the blister half-width, h is the total film thickness, and B is the unit width, which cancels when multiplied by the transformed moment of inertia [9]. The residual stress can then be determined from the blister height and delamination stress as follows [11],

$$\sigma_r = \sigma_b\left(\frac{3\delta^2}{4h^2}+1\right) \tag{2}$$

where δ is the buckle height and σ_r is the average residual stress in the film given by [9],

$$\sigma_r = \sigma_{rAu}\left(\frac{h_{Au}}{h}\right)+\sigma_{rW}\left(\frac{h_W}{h}\right) \tag{3}$$

Under steady state conditions, the width of the telephone cord blister remains fixed creating a straight-sided blister with growth occurring along the more or less circular front. This gives a steady state fracture energy, Γ_{SS}, as follows [11],

$$\Gamma_{ss} = \left[\frac{\left(1-\bar{\nu}^2\right)h\sigma_r^2}{2\bar{E}}\right]\left(1-\frac{\sigma_b}{\sigma_r}\right)^2 \tag{4}$$

where h , $\bar{E}$ and $\bar{\nu}$ are the multilayer film thickness, and thickness weighted elastic modulus and Poisson's ratios respectively.

Using optical microscopy and atomic force microscopy, the buckle heights and widths were measured across numerous telephone cord blisters and used to calculate the delamination and residual stresses from equations (1) and (2). The residual stress were found be to be -2.1 GPa in the total film system giving a residual stress in the tungsten overlayer of -2.6 GPa. This value is in good agreement with wafer curvature measurements of -2.3 GPa used to establish the deposition parameters and supports the use of this approach in determining fracture energies. The residual and delamination stresses were then used to calculate a steady state fracture energy of of 6.7 J/m^2 in this film system.

Failure in the gold-2w/o-copper films required nanoindentation to trigger delamination and circular blister formation. In all blisters, the center is constrained giving rise to a reverse or double buckle configuration. Following the analyses of Marshall and Evans [12] and Evans and Hutchinson [13], the delamination stress is given by,

$$\sigma_b = \frac{k}{Bha^2}\left[\frac{E_{Au}}{\left(1-\nu_{Au}^2\right)}\right]\left(I_T\right) \tag{5}$$

where a is the blister radius and k is equal to 14.68. The stress from indentation is given as follows [12,13],

$$\sigma_V = \frac{\bar{E}V}{2\pi\left(1-\bar{\nu}\right)a^2h} \tag{6}$$

V is the displaced indent volume contributing to in-plane stresses. Previous work [14] on tantalum nitride films and analysis of indents in the gold-2w/o-copper films shows that 60 percent of measured displaced indent volume contributes to in-plane stresses. The corresponding strain energy release rate for circular blister formation due to residual and indentation stresses, $G(\alpha)$, is given by

$$G(\alpha) = \frac{(1-\bar{\nu}^2)h\sigma_V^2}{2\bar{E}} + (1-\alpha)\frac{(1-\bar{\nu})h\sigma_r^2}{\bar{E}} - (1-\alpha)\frac{(1-\bar{\nu})h(\sigma_V-\sigma_b)^2}{\bar{E}} \tag{7}$$

Combining blister diameter and indent displacement volume measurements with residual stress levels determined from gold-on-copper blister films, an average fracture energy of 7.2 J/m^2 was calculated from equation (7). The uniform width and circular blister fracture energies are mixed mode values consisting of shear and normal contributions. The normal contribution is critical to understanding mechanisms controlling susceptibility to interfacial fracture. Of the criteria proposed to describe the relationship between mixed mode and mode I contributions, $\Gamma_I=\Gamma(\Psi)/[1+\tan^2\{(1-\lambda)\Psi\}]$ is most often used. In this expression, λ is a material parameter equal to 0.3 for most materials and Ψ is the phase angle of loading described in previous work. [11,15] This expression was then used to calculate the mode I fracture energies for both film systems. Average blister widths and diameters, delamination stresses, residual stresses, mixed mode and mode I fracture energies, and phase angles of loading are given in Table I for the uniform width blisters in as-deposited gold-on-copper films and the circular blisters in the gold-2w/o-copper films. Also included are results for thin gold films for comparison. The fracture energies were significantly higher for gold-2w/o-copper than the gold-on-copper films. The gold-on-copper fracture energies are in agreement with literature values for copper on sapphire at the same thickness. The fracture energies are also consistent with the better durability during handling and testing exhibited by the gold-copper alloy films. It is unlikely that the gold-2w/o-copper alloy film would have higher bond strength than its constituent elements. This suggests that the higher fracture energy for the alloy film lies with film energy dissipation processes.

Working from the relationship for crack initiation strain energy derived by Mao [16], Volinsky et al. [17] showed that interfacial bond strength is directly related to yield strength of the film and crack initiation strain energy release rate as follows,

$$\sigma_{bond} = \left[\left(\frac{8}{3}\right)\left(\frac{E\,G_o}{\sigma_{ys}h}\right)\right]^{1/2} \tag{8}$$

In this equation, σ_{bond} is the interfacial bond strength, G_o is the crack initiation strain energy release rate, μ is the shear modulus, and σ_{ys} is the yield strength. Bond strengths were then calculated setting the strain energy release rate equal to the mode I fracture energies and using the Tabor relationship of H/3 to define yield strength. The results are given in Table I and show that the bond strength of copper to sapphire and gold-2w/o-copper on sapphire are essentially equal. They are also significantly higher than observed for thin gold films. This strongly suggests that the higher fracture energy measured for the gold-2w/o-copper on sapphire films was due to solid solution hardening effects on deformation and not compositional effects on adhesion. The results are also consistent with the conclusions of Volinsky and coworkers [17] that deformation makes a significant contribution to measured fracture energies in 200-nm-thick films.

CONCLUSIONS

In this study, highly compressed overlayers were combined with nanoindentation to study the effects of copper on susceptibility to interfacial fracture of gold-on-copper and gold-2w/o-copper alloy films. Highly stressed tungsten overlayers were combined with nanoindentation to induce delamination and blister formation from which fracture energies were determined. The results on as-deposited films showed that the fracture energies for the gold-copper alloy film were higher than the gold-on-copper films. The fracture energies were consistent with the better durability exhibited during handling and testing by the gold-copper alloy films. However, interfacial bond strengths were essentially equal. This strongly suggests that the fracture energies are comprised of significant contributions from plastic deformation processes and that the higher fracture energy measured for the gold-2w/o-copper film was due to solid solution hardening.

ACKNOWLEDGMENTS

The authors gratefully acknowledge the technical assistance of M. Clift and J. Chames of Sandia National Laboratories in Livermore, CA and the support of the U.S. DOE through Contract DE-AC04-94AL85000.

Table I. Average blister heights and widths, stresses, fracture energies, and bond strengths are given gold-on-copper and gold-2w/o-copper films. Data for gold films are also included for comparison.

Film	h_{Au} (nm)	h_W (nm)	b,a (□m)	$□_b$ (GPa)	$□_V$ (GPa)	$□_r$ (GPa)	$□_{ss}$,□(□) (J/m^2)	□	$□_I$ (J/m^2)	□ (GPa)	$□_{bond}$ (GPa)
Au	200	200	16.4	0.08	--	-1.7	1.8	-79	0.6	2.2	2.3
Au-Cu	200	840	83.2	0.05	--	-2.1	6.7	-79	2.2	2.2	5.5
Au2Cu	200	840	11.3	3.06	-1.1	-2.1	7.2	-69	3.2	3.0	5.7

REFERENCES

1. K. L. Mittal, *Electrocomponent Science and Technology*. **3**, 21 (1976).
2. D. M. Mattox, *Thin Solid Films*. **18**, 173 (1973).
3. P. M. Hall, J. M. Morabito, and N. T. Panousis, *Thin Solid Films*, **41** 341 (1977).
4. L. G. Feinstein and J. B. Bindell, Thin Solid Films, 62, 37 (1979).
5. P. M. Hall, N. T. Panousis, and P. R. Menzel, *IEEE Trans. Parts, Hybrids, Packag.*, **PHP-11**, 202 (1975).
6. Y. Wei and J. W. Hutchinson, *Int'l. Journal of Fracture*, **9**, 315 (1998).
7. A. Bagchi and A. G. Evans, *Thin Solid Films*, **286**, 203 (1996).
8. A. Bagchi, G. E. Lucas, Z. Suo, and A. G. Evans, *J. Mater. Res*., **9**, 1734 (1994).
9. M. D. Kriese, W. W. Gerberich, and N. R. Moody, *J. Mater. Res*., **14**, 3007 (1999).
10. M. D. Kriese, N. R. Moody, and W. W. Gerberich, *Acta mater*., **46**, 6623 (1998).
11. J. W. Hutchinson and Z. Suo, in *Advances in Applied Mechanics*, edited by J. W. Hutchinson and T. Y. Wu (Academic Press Inc., vol. **29**, New York 1992) pp. 63-191.
12. D. B. Marshall and A. G. Evans, *J. Appl. Phys*., **56**, 2632 (1984).
13. A. G. Evans and J. W. Hutchinson, *Int. J. Solids Struct*., **20**, 455 (1984).
14. N. R. Moody, R. Q. Hwang, S. Venkataraman, J. E. Angelo, D. P. Norwood, and W. W. Gerberich, *Acta mater*. **46**, 585 (1998).
15. M. D. Thouless, J. W. Hutchinson, and E. G. Liniger, *Acta metall. mater*. **40**, 2639 (1992).
16. S. X. Mao and A. G. Evans, *Acta Mater*., **45**, 4263 (1997).
17 A. A. Volinsky, N. I. Tymiak, M. D. Kriese, W. W. Gerberich, and J. W. Hutchinson, in *Fracture and Ductile vs Brittle Behavior-Theory, Modeling, and Experiment*, edited by G. E. Beltz, R. L. Blumberg Selinger, M. P. Marder, and K-S. Kim (Mater. Res. Soc. Proc**. 539**, Pittsburgh, PA 1999) pp. 277-290.